Nonlinear optical properties of GaAs/GaAlAs multiple quantum well material: phenomena and applications

D. S. Chemla
A. B. Miller
AT&T Bell Laboratories
Holmdel, New Jersey 07733

P. W. Smith
Bell Communications Research, Inc.
Holmdel, New Jersey 07733

Abstract. Semiconductor microstructures whose dimensions are comparable to atomic dimensions and whose interfaces are atomically smooth exhibit novel optical properties not encountered in the parent compounds. Quantum well structures, which consist of ultrathin semiconductor layers alternately grown one on the other, possess remarkable optical nolinearities and electro-optical properties with potential applications in optoelectronics. In this paper we review our studies of GaAs/AlGaAs quantum well structures (QWS). We briefly discuss the physics of absorption in QWS at room temperature, and we describe the mechanisms of saturation of excitonic absorption and refraction and that of electroabsorption in QWS. Finally, we review the applications of these effects to optical processing and optoelectronic devices.

Subject terms: nonlinear optics; electroabsorption; multiple quantum wells.

Optical Engineering 24(4), 556-564 (July/August 1985).

CONTENTS

1. INTRODUCTION

In recent years there have been a number of trends that lead one to predict that optical switching and signal processing elements are likely to become important components in future communications and information processing systems. In communications, the demand for ever-increasing bit rates has resulted in a rapid conversion to optical fibers as the transmission medium. In these optical communications systems, the capacity is limited by the capability of the electronics to handle high bit rates. It is tempting to suggest that the use of optical signal processing elements would dramatically increase the capacity of such systems. In the area of computing, there is much interest in parallel architectures that permit high throughput. Again, the capabilities of optics for parallel information processing indicate that optical devices may find important applications in this area.

In order for any of these applications to become practical, a suitable nonlinear material must be found to form the basis of these optical devices. Such a material must have a number of desirable characteristics: the nonlinear effects must be large and should also have fast response times so that devices can run with low operating energies; the material must be stable and robust, with good optical quality and resistance to optical damage. It also would be desirable for the material and effects to be compatible with the other technologies with which they must interface. The interface with electronics is most obvious. For communications applications, compatibility with laser diodes also would be desirable, and even in other applications there must be compatibility with some convenient light source. An ideal material would enable us to perform electronic, optical, and optoelectronic functions all on the same chip.

In this paper we describe our studies of GaAs/GaAlAs multiple quantum well (MQW) material, which to date appears to be the best material in terms of satisfying the criteria in the previous paragraph. Furthermore, it offers two completely different types of nonlinear effects: nonlinear optical phenomena associated with absorption saturation and a novel electroabsorption mechanism.

Central to all of these phenomena is the fact that MQW structures exhibit exciton resonances (sharp absorption features near the optical band edge) *at room temperature*. First, we will briefly discuss the physics of this linear absorption phenomenon in Sec. 2 of the paper. Then in Sec. 3 we will describe the mechanisms of the nonlinear absorption and refraction at these resonances. In Sec. 4 principles of the electroabsorptive effects will be covered, and in Sec. 5 the applications of all these effects will be reviewed. Several important applications have already been demonstrated, and recent experiments have pointed the way to wider applicability.

2. LINEAR ABSORPTION IN QUANTUM WELL STRUCTURES

At low temperatures in bulk semiconductors the absorption near the fundamental edge is governed by exitonic effects.[1] Excitons are electron-hole (e-h) pairs forming a bound state analogous to the

Invited Paper NO-101 received Jan. 15, 1985; accepted for publication Jan. 28, 1985; received by Managing Editor April 15, 1985.

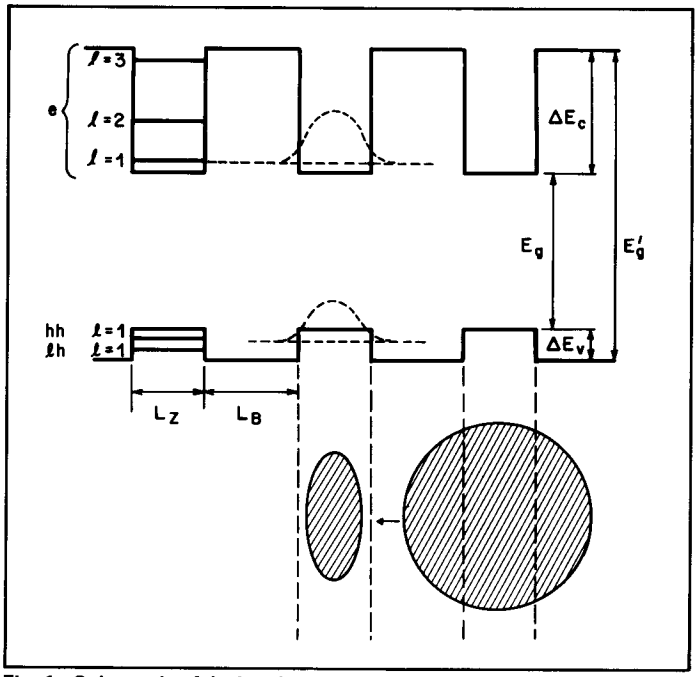

Fig. 1. Schematic of the band structure of a multiple quantum well structure along the normal to the layers (z) in real space. The dashed line represents the electron and the hole wave functions along z. The striped circle and ellipse illustrate how the exciton is compressed by the confinement.

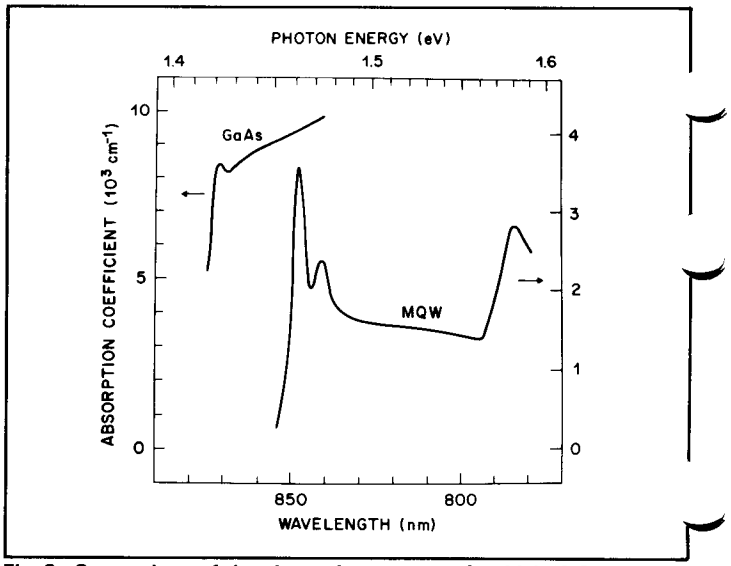

Fig. 2. Comparison of the absorption spectra of a thick (3.2 μm) high quality GaAs sample of a multiple quantum well structure consisting of 77 periods of 102 Å GaAs layers alternating with 207 Å AlGaAs layers.

hydrogen atom. They produce very sharp resonance peaks just below the band gap, where a large oscillator strength is concentrated in a narrow spectral domain. Note that these resonances correspond to the *creation* of excitons, not the excitation of existing particles; a good analogy is the creation of positronium atoms in a vacuum by a photon. The excitonic resonances have been extensively investigated in linear[2] and nonlinear optics,[3] but so far they have have not been used for applications because of the low temperature at which they are usually observed. The physical mechanism that prevents observation of exciton resonances at room temperature is that, in polar semiconductors, longitudinal-optic (LO) vibrations produce strong electric fields that ionize the weakly bound excitons.

In recent years modern techniques of crystal growth have enabled us to fabricate semiconductor heterojunctions that are smooth down to one atomic monolayer with almost perfectly controlled composition.[4] Using pairs of semiconductors with very specific physical and chemical compatibility, it is possible to grow alternate ultrathin layers of each compound to form MQW structures.[5] Examples of these structures have been made using III-V and II-VI semiconductors.[6]

Because of the band gap difference between the two components, the e-h pairs are confined in the low gap layers. The motion of the carriers has to be quantized both along the normal to the layers (z) and in the plane (x,y). For ultrathin layers with thickness $L_z \sim$ 100 Å the confinement along z produces a series of discrete states, whereas the particles are free to move in the x-y plane (Fig. 1). This confers to the e-h gas a quasi two-dimensional character that has recently attracted much attention.[7]

The effect of the confinement on the density of states that describe the optical transitions is to transform the usual parabolic edge into a series of steps. It also raises the degeneracy of the upper valence band of III-V semiconductors by introducing a splitting between the heavy and the light holes. The electron and holes still interact through the Coulomb interaction, but in MQW structures the e-h bound states are flattened, the average distance between the two particles is reduced, and the exciton binding energy is increased, resulting in enhanced excitonic effects.[5,8] In fact, because MQW structures have two valence subbands at each absorption edge, two excitons can be seen involving the heavy and the light hole, respectively. However, although the exciton binding energy is increased in the MQW structures, the interaction with the phonons is almost unaffected for two reasons. First, the pair of compounds that form an MQW structure usually have very similar phonon spectra, and in addition the quasi two-dimensional excitons are mostly localized in the low gap layers and thus do not significantly probe the other compound.[9] This is enough to produce sharp excitonic resonances at room temperature in the absorption spectra of high quality GaAs/AlGaAs[10] and GaInAs/AlInAs MQW structures,[11] as shown, for example, in Fig. 2. However, it should be noted that at room temperature the excitons live just long enough to produce these beautiful resonances; because the energy of the LO-phonons is much larger than the binding energy, the excitons are very promptly ionized. Line shape studies as a function of temperature show that the mean time for thermal phonon ionization is 0.4 ps for GaAs MQW structures[12] and 0.24 ps for GaInAs MQW structures.[11] This remarkable property is at the origin of some of the very interesting properties that are reviewed in this paper.

3. NONLINEAR ABSORPTION AND REFRACTION

When free e-h pairs or excitons are generated, they induce changes in the absorption coefficient and in the refractive indices. The physical mechanisms involved are (a) the screening of the Coulomb interaction and (b) phase-space filling.[13] Screening by free e-h pairs is much more efficient than that due to excitons. In both cases it produces a red shift of the band gap, whereas the absolute energy of the exciton is not significantly changed due to its electric neutrality. As the band gap diminishes, the exciton binding energy reduces, it loses oscillator strength, and it eventually disappears.[13] Such a behavior is shown in Fig. 3 for an MQW structure that consists of 65 periods of GaAs layers 96 Å thick and AlGaAs layers 98 Å thick.[14] Two absorption spectra are presented. The dashed line gives the absorption of the unperturbed sample; the solid line gives the absorption when the sample is excited by a cw laser diode delivering 5 mW at 831 nm and focused to give an intensity of 800 W/cm^2 in the sample. Under this nonresonant excitation, free e-h pairs are directly generated that effectively screen the Coulomb interaction so that the two exciton peaks have disappeared, leaving only the renormalized step-like continuum. The same effects are expected to be seen in resonant excitation with cw or even ps laser sources because the excitons are ionized by thermal phonons in less than 0.5 ps and in turn generate free e-h pairs. Measurements of the changes in magnitude of the

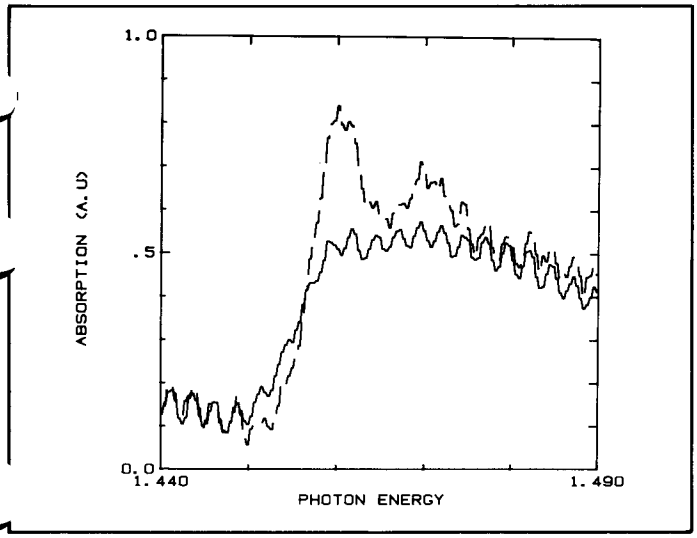

Fig. 3. Effect of free carriers, generated by a cw laser diode delivering 800 W/cm² at 831 nm, on the absorption spectrum of an MQW structure. (The ripples on the spectra are Fabry-Perot fringes in the quartz plate supporting the sample.)

absorption at the exciton peak for the MQW structure and the thick GaAs samples whose spectra were compared in Fig. 2 are shown in Fig. 4.[12] The solid lines are semiempirical fits with two saturable species, one representing the exciton and the other representing the renormalized band gap as it shifts down to the exciton original position. For GaAs the fit gives a constant (not saturable) background and a saturable species with a saturation intensity of 4.4 kW/cm²; for the MQW structure the exciton saturation intensity is as low as $I_s = 580$ W/cm². The very low saturation intensity of quasi two-dimensional excitons is well accounted for by a model based on the many-body theory of free carrier screening.[15] The value of I_s corresponds to carrier densities such that there is a probability ~½ of finding an electron or a hole in a excitonic area. This is in good agreement with the intuitive picture of the screening of a bound pair by free e-h pairs. Studies of nonlinear absorption and four-wave mixing using picosecond pump-probe techniques have confirmed these results.[16] To be more quantitative, let us write the intensity-dependent absorption coefficient and refractive index as

$$\alpha(I) = \alpha_0 + \alpha_2 I = \alpha_0 + \sigma_{eh} N \ , \quad (1)$$

$$n(I) = n_0 + n_2 I = n_0 + n_{eh} N \ , \quad (2)$$

where I is the light intensity and N is the carrier concentration; our measurements give $\alpha_2 = 40$ cm/W or $\sigma_{eh} = 7\times10^{-14}$cm² and $n_2 = 2\times10^{-4}$ cm²/W or $n_{eh} = 3.7\times10^{-19}$ cm³. This corresponds in the formalism of nonlinear susceptibilities to the very large value $\chi^{(3)} = 6\times10^{-2}$ esu, i.e., several orders of magnitude larger than that usually encountered in semiconductors even at low temperature.

The changes in absorption induced by the e-h gas last until the carriers recombine, i.e., approximately 30 ns.[14,16] However, MQW structures also present a new nonlinear process with a very fast recovery time. It is often stated that excitons are bosons and, therefore, that they cannot saturate. This is not correct; excitons are composite bosons formed of two fermions. In the limit of very small density, they are so far apart that the exclusion principle is not effective; as they become more densely packed, each particle within an exciton can interact with the particles that compose the nearby excitons, and saturation effects become visible. The direct generation of excitons therefore produces effects that are qualitatively different from those due to the creation of free e-h pairs. Since at room temperature excitons live a fraction of a picosecond before being ionized, it should be possible to observe in the absorption spectrum

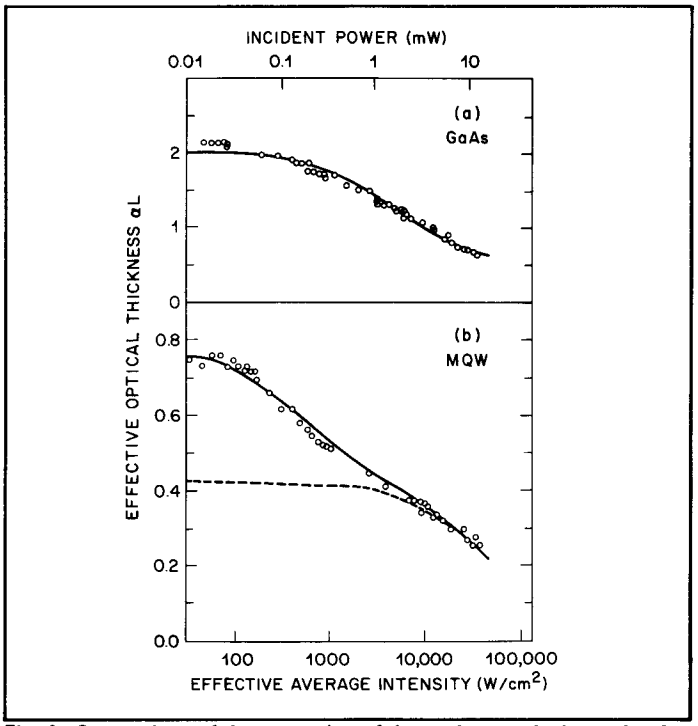

Fig. 4. Comparison of the saturation of the exciton peak absorption for the GaAs and the MQW samples whose absorption spectra are shown in Fig. 2.

the dynamics of the transformation of excitons into free pairs. The recently developed femtosecond spectroscopic techniques now provide the required time resolution.[17]

Using a two-continuum pump-probe system capable of a 150 fs time resolution,[18] the ionization of room-temperature excitons has been observed directly.[19,20] In these experiments the effects on the absorption spectra of resonantly generated excitons have been compared to those of free e-h pairs directly created in the continuum. For nonresonant pumping all the changes follow a smooth variation proportional to the integral of the pump pulse, and at long times ($t > 1$ ps) they reproduce the changes observed with cw excitation. Conversely, for resonant pumping an almost instantaneous bleaching of the exciton peak is seen, which transforms in about half a picosecond into the change observed in the nonresonant case. The dynamics of the absorption at the exciton peak are shown in Fig. 5 for the two cases. These data yield a mean time for ionization by thermal phonons of 300 ± 100 fs, in excellent agreement with the lifetime deduced from the line width measurments.

The description of the effect of resonant generation of excitons on the absorption requires a many-exciton formalism that is quite elaborate.[13] Excitonic states are built from single particle states of the crystal, and it can be shown that the volume of the phase space that an exciton "occupies" is proportional to the square of the Fourier transform of its wave function in real space.[13] The case of quasi two-dimensional excitons in MQW structures has been quantitatively analyzed.[21] A simple and pictorial way to interpret these calculations is to consider that every exciton uses in real space a small area of the MQW structure that cannot support another exciton. It turns out that this area is approximately four times the area defined by the Bohr radius of the exciton, in excellent agreement with the experimental data.

The dynamics of room-temperature excitons introduce a new concept in nonlinear optics. It is often believed that very large nonlinear cross sections are always accompanied by slow responses. In the case of room-temperature excitons, we have two species; one (the free e-h pairs) has a long lifetime, but the other (the excitons) is unstable and transforms into the former in a very short time. Because the two species have significantly different cross sections, the overall

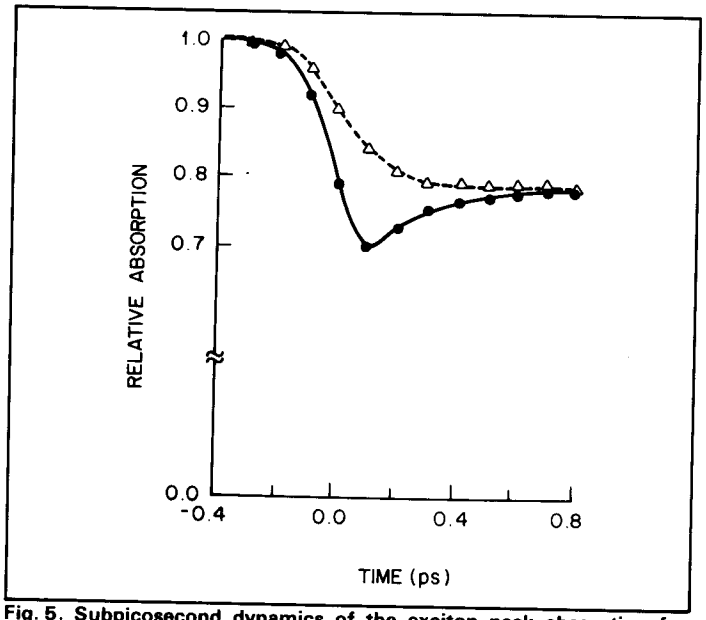

Fig. 5. Subpicosecond dynamics of the exciton peak absorption for resonant (solid line) and nonresonant (dashed line) excitation with 150 fs pulses.

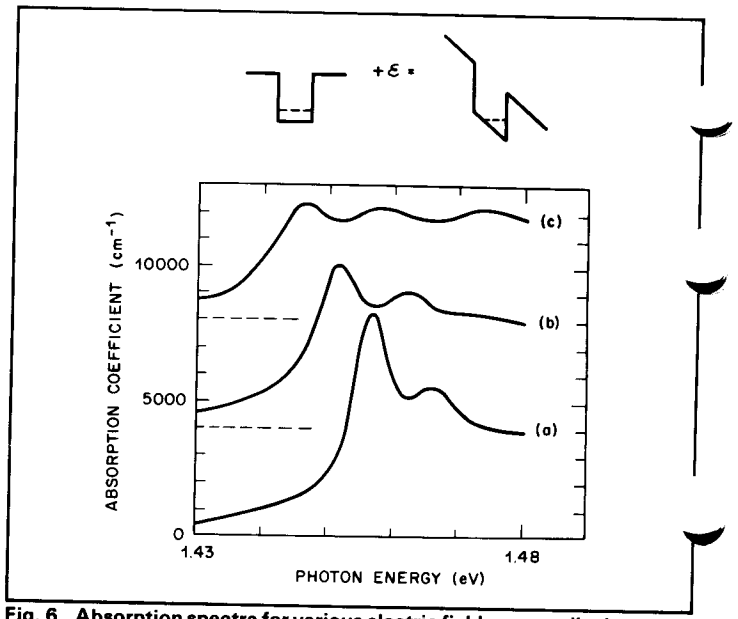

Fig. 6. Absorption spectra for various electric fields perpendicular to the quantum well layers. (a) 1×10^4 V/cm; (b) 4.7×10^4 V/cm; (c) 7.3×10^4 V/cm. The zeros of the spectra are displaced for clarity. The inset illustrates the effect of a static field on the potential seen by the carriers.

response of the medium presents a strong nonlinear effect with a fast partial recovery. This new and most unusual feature may have novel applications.

4. ELECTRIC FIELD EFFECTS

So far we have discussed the linear absorption in MQW structures and the nonlinear effects of optically adding electrons and holes and/or excitons. MQW structures also show some interesting effects, again on the absorption spectra near the band edge, when electric fields are applied to the material. One such novel effect, called the quantum-confined Stark effect (QCSE),[22] is both large and fast and already has demonstrated interesting device potential.[23-26] The devices will be discussed in Sec. 5; here we will briefly discuss the effect itself. One important aspect of the effect is that it appears to rely on the confinement of the carriers within the thin semiconductor layers; thus, it is truly a quantum well effect and will not exist in bulk semiconductors at any temperature. The existence of excitons may, however, be important for the QCSE; again, the observation of room-temperature excitons is important to make this effect of greater practical utility.

Conventional semiconductors show an effect known as the Franz-Keldysh effect when electric fields are applied.[27] This results in a slight shift of the absorption edge to lower photon energies, but the predominant consequence is really a broadening of the edge. Modulators have been successfully demonstrated using this effect. They usually involve lengths of hundreds of micrometers since they operate well down in the tail of the band edge absorption where the broadening of the edge results in large relative changes of absorption (of the order of 100 cm^{-1}). In conventional semiconductors, exciton resonances are not normally directly relevant in such devices at room temperature because they are not resolvable. However, if the semiconductor is cooled so that the excitons can be seen, then the broadening becomes particularly apparent on the exciton resonances themselves.* This broadening can be simply understood as field ionization of the excitons; no sooner is the exciton created than it is ripped apart by the strong electric field. The field ionization therefore shortens the lifetime of the exciton, thereby broadening the absorption line. The exciton does start to show some shift to lower energies; this shift is actually exactly analogous to the Stark shift of the ground state of a hydrogen atom. However, this shift is limited to about 10% of the binding energy of the hydrogenic system (of the order of 1 meV for typical exciton binding energies) at a few times the classical ionization field. After this point the field ionization is so rapid that the hydrogenic system no longer exists as a quasi-bound system, and the resonance is no longer resolvable. Other physical mechanisms take over after this, and these do not show the same shifting behavior. In fact, they can actually show shifts of the opposite sign.[28]

When we apply fields parallel to the quantum well layers, we find effects similar to those expected in low temperature conventional semiconductors, only now we can see these at room temperature; the exciton progressively broadens and disappears with increasing field.[29] This effect may be understood through the same field ionization mechanism as for conventional semiconductors. Because it can be seen at room temperature, this effect may also be useful.

However, when we apply the field perpendicular to the layers, we see a qualitatively different phenomenon; the excitons shift to lower photon energies, with little or no broadening up to very high fields. A typical set of absorption spectra with increasing field is shown in Fig. 6.

The explanation of this effect is essentially that the potential barriers inhibit the field ionization of the exciton, hence inhibiting the broadening mechanism. Consequently, we can apply fields that would normally completely destroy the exciton resonance, but because the particle continues to exist, the Stark shift continues up to much larger values than are possible for conventional hydrogenic systems. We measure shifts of 2.5 time the binding energy at 50 times the classical ionization field.

There are two different ways in which the potential barriers inhibit the field ionization, both of which are important for the QCSE. First, the walls of the potential wells inhibit the electrons and holes from tunneling totally away from one another. Second, because the wells are narrow (e.g., 100 Å) compared to the conventional exciton diameter (300 Å), even when the electron and hole are pulled to opposite sides of the well the Coulomb interaction between them is still strong, and the exciton is still a strongly bound particle. (If, for example, the wells were 1000 Å wide, the exciton could be effectively field-ionized even if the electron and hole never left the well.) The resulting effect is still really a Stark effect, but the quantum confinement has qualitatively changed the behavior, hence, the title of quantum-confined Stark effect.

*For a comprehensive theoretical discussion of exciton broadening with field and the Franz-Keldysh effect, see Ref. 28.

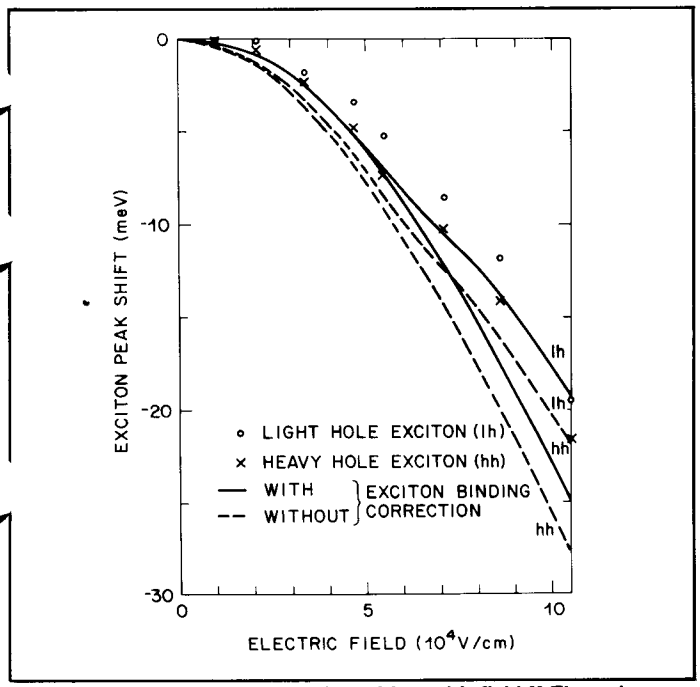

Fig. 7. Shifts of the exciton peak position with field.[22] The points are experimental and the lines are theoretical. There are no fitted parameters in the theory.

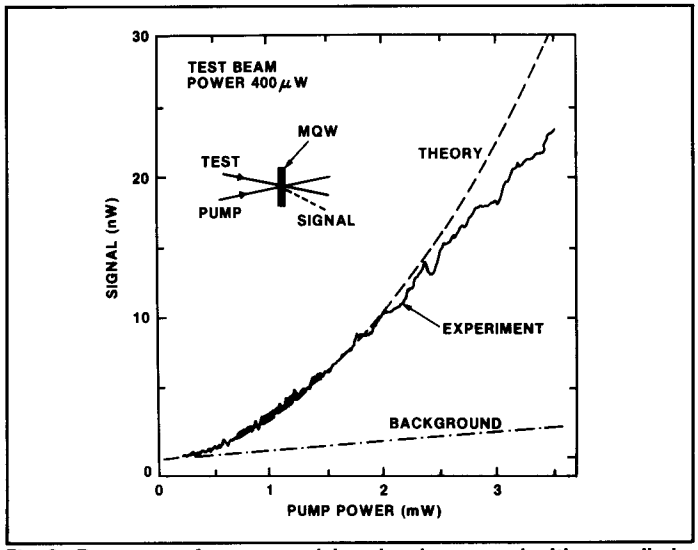

Fig. 8. Degenerate four-wave mixing signal measured with a cw diode laser light source. The dashed line is a theoretical fit showing quadratic behavior up to ~2 mW with a small linear background (shown separately as the dotted-dashed line). Saturation of the nonlinearity at higher pump powers shows up as a deviation from the theoretical curve.

The modeling of the QCSE is done by considering a hydrogenic system in a potential well. In principle, therefore, the model is applicable to other hydrogenic systems, although the fields and confinements required to demonstrate the QCSE in the hydrogen atom itself are not readily attainable. The same effect should, however, be observable in other confined excitonic systems.

The results of the theoretical calculations and the experimentally measured shifts are shown in Fig. 7. As an approximation, the calculated shifts can be separated into contributions from (a) the change in energy from the individual electron and hole each being pulled to the side of the well (the "single particle" shifts) and (b) the energy change from the electron and hole being pulled away from each other (the "exciton binding" shift). The single particle shifts are usually dominant, although the exciton binding correction is important at low fields.

The ultimate speed of the QCSE has not been measured so far; it has, however, been tested down to 100 ps.[25] The practical limits on response times so far have been the RC time constants of the package; the fundamental limit appears to be the speed at which the quantum-mechanical wave function can respond, which is limited by the uncertainty principle to times less than or of the order of 1 ps. The speed is not limited by carrier lifetimes.

5. APPLICATIONS

5.1. Four-wave mixing

The first studies of nonlinear refractive index effects in MQW samples were performed with a forward degenerate four-wave mixing experiment.[16] The MQW sample was 1.26 μm thick with sixty-five 76 Å GaAs quantum wells. A diffraction efficiency of $\sim 10^{-4}$ was observed with ~30 W/cm^2 average intensity from a mode-locked laser. From measurements of the absorption change induced in a probe beam by a strong pump beam (the nonlinear absorption) and the four-wave mixing signal as function of wavelength, it was possible to deduce the refractive index change as a function of wavelength. The measured nonlinear refractive index and absorption coefficients are given in Sec. 3. The values are sufficiently large to permit strong nonlinear effects to be observed with laser diodes as the sole light source. This, in fact, has been demonstrated for the four-wave mixing experiment, and good results were obtained (Fig. 8) with milliwatt power levels.[30] This is the first demonstration of a nonlinear optical device driven with a low power cw semiconductor diode laser.

5.2. Mode-locking

A number of techniques have been tried for mode-locking semiconductor diode lasers. Although some success has been demonstrated with active mode-locking techniques, it is known from dye laser research that far shorter pulses are obtained with passive mode-locking techniques using a saturable absorber within the laser resonator.

Previous attempts to mode-lock diode lasers with saturable absorbers have used absorption produced by optical damage. By aging a laser to the point of severe degradation, pulses as short as 5 ps were observed for a short time before laser failures.[31] Bursts of sub-ps pulses have been produced using aged lasers[32] or lasers with proton-bombarded end facets.[33] Recently, 35 ps pulses have been produced in a GaAs laser with uniform current injection.[34]

The characteristics of the ideal saturable absorber for laser diode mode-locking can be deduced from theoretical studies of mode-locking.[35,36] Such an absorber should saturate at low light intensities and recover rapidly when the light is removed. Expressed mathematically, these criteria become

$$\frac{\sigma_A}{A_A} > \frac{\sigma_g}{A_g}\,, \tag{3}$$

$$\tau_A < \tau_g\,, \tag{4}$$

where σ_A and σ_g are the cross sections for the absorber and the gain, respectively, A_A and A_g are the cross sections of the laser beam in the absorber and the gain, and τ_A and τ_g are the lifetimes of the light-induced saturation of the absorber and gain.

It is clear from Sec. 2 that GaAs/GaAlAs MQW material has a much larger cross section than the bulk GaAs that characterizes the gain of a GaAs laser diode. The absorber recovery time (30 ns), however, is substantially longer than the gain recovery time (~400 ps). In order to use this material to passively mode-lock a GaAs laser, it is necessary to speed up the absorber recovery time substantially.

One way to obtain a fast recovery time is to utilize carrier diffusion. Because the MQW absorption saturation is due to screening by optically excited carriers, carrier diffusion out of the excited region results in recovery of the absorption. From our measurements of

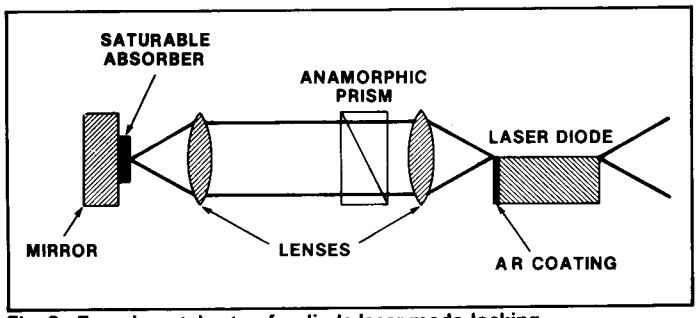

Fig. 9. Experimental setup for diode laser mode-locking.

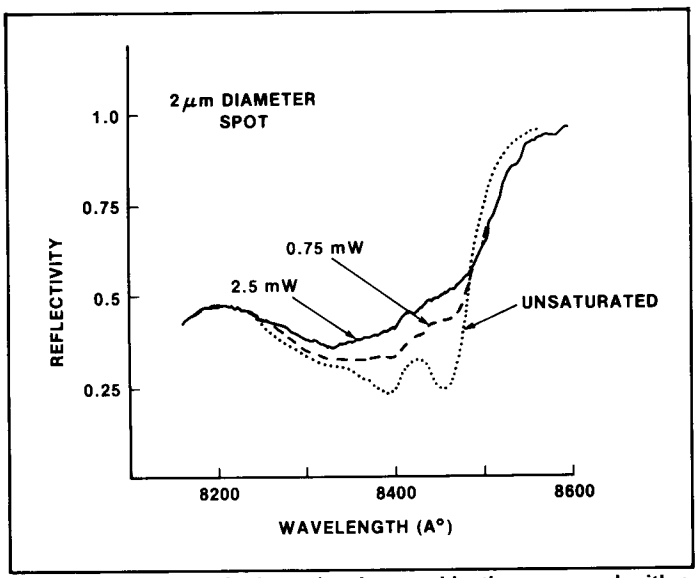

Fig. 10. Reflectivity of mirror-absorber combination measured with a tunable dye laser as a function of wavelength.

absorption recovery versus spot size, we find

$$\tau = \frac{r^2}{C}, \tag{5}$$

where τ is the absorption recovery time for an excited spot of radius r, and $C = \gamma D$, where D is the diffusion constant and γ is a geometrical constant that depends on the beam shape. Our measurements give a value for C of 10 $\mu m^2/ns$ for Gaussian beams in GaAs MQW material. Thus, with a beam focused to $r = 1$ μm, we expect $\tau = 100$ ps, which is fast enough to satisfy Eq. (4).

Experiments were performed using the setup shown in Fig. 9.[37] A Hitachi HLP-1400 GaAs laser was modified by applying an antireflection coating to one facet. The remaining reflectivity was $<10^{-3}$. An anamorphic prism was used to convert the elliptical laser beam to one with an approximately circular cross section so that tighter focusing on the absorber could be obtained. The MQW absorber consisted of 47 periods of 98 Å GaAs layers alternated with 99 Å of $Ga_{0.71}Al_{0.29}As$ layers grown by molecular beam epitaxy on top of a 1 μm GaAlAs etch-stop layer on a GaAs substrate. This sample was epoxied to a high reflectivity dielectric mirror on a sapphire substrate. The GaAs substrate was removed with a selective etch. The exposed surface of the MQW absorber was then antireflection coated. The reflectivity of the mirror-absorber combination as a function of wavelength is shown in Fig. 10. The observed saturation is in good agreement with transmission measurements. The unsaturated reflectivity of the mirror-absorber combination was 0.25 at the peak of the exciton resonance (8460 Å), and it increased to ~0.5 at 2.5 mW, which corresponds to the average power level in the laser under mode-locked conditions.

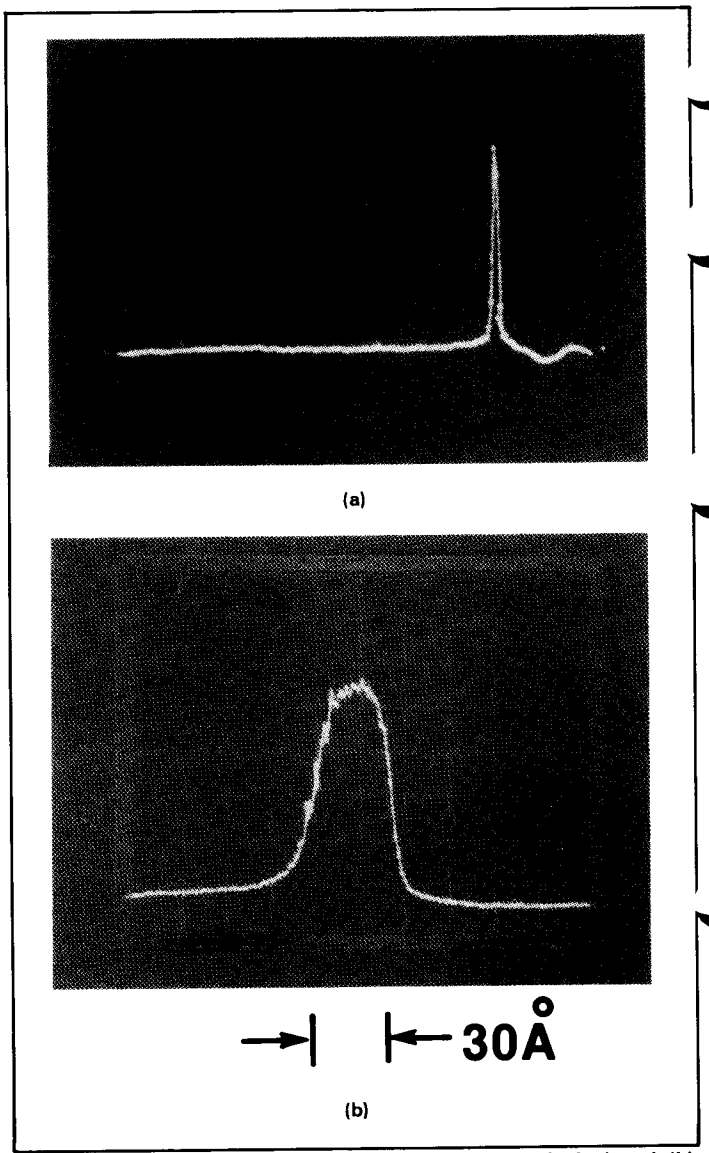

Fig. 11. Laser output spectrum under (a) non-mode-locked and (b) mode-locked conditions. The total wavelength scan is 200 Å in both cases.

An 8 mm lens was used to focus the light to a spot size of $r \sim 1$ μm on the MQW absorber. The total length of the laser was ~30 cm. By making a small change in the lens-absorber spacing, the chromatic aberration of the lens-prism combination could be used to tune the laser output over a wide spectral range. The output light from the rear facet of the laser diode was simultaneously monitored with a fast photodiode, an optical multichannel spectrum analyzer, and an optical autocorrelator.

Stable mode-locking was obtained at currents near laser threshold. The average output power was ~1 mW. Both single and double pulsing per transit time could be achieved, i.e., pulse repetition rates of ~0.5 or ~1 GHz. The width of the output spectrum was observed to increase dramatically under mode-locked conditions. Figure 11 shows that a featureless band ~30 Å wide is obtained.

In order to measure the true width of the mode-locked pulses, it is necessary to use an autocorrelation technique. This technique involves splitting the pulse train, recombining the two beams in a nonlinear crystal, and measuring the second harmonic light signal as a function of the time delay between the arrival of the pulses in each beam. Incomplete mode-locking results in 50 to 100 ps pulses; the autocorrelation trace is characterized by many coherence spikes spaced by ~8 ps. This time corresponds to the round-trip time in the

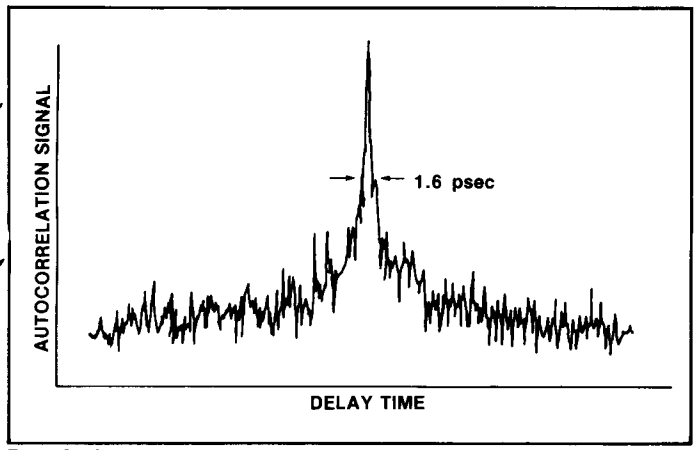

Fig. 12. Autocorrelation trace of 1.6 ps mode-locked pulse train.

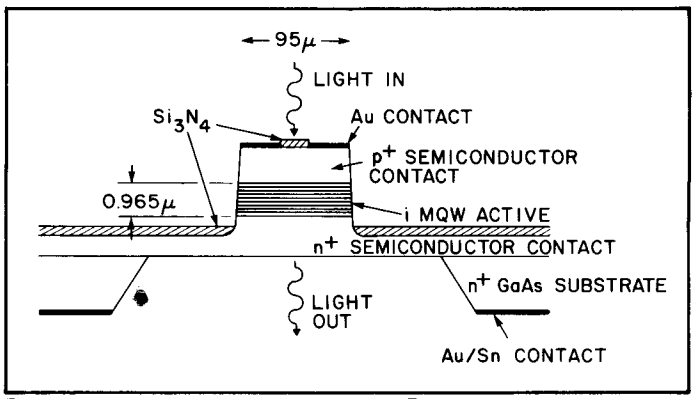

Fig. 13. Schematic view of modulator.[25] For details of layer thickness and compositions, see Ref. 23.

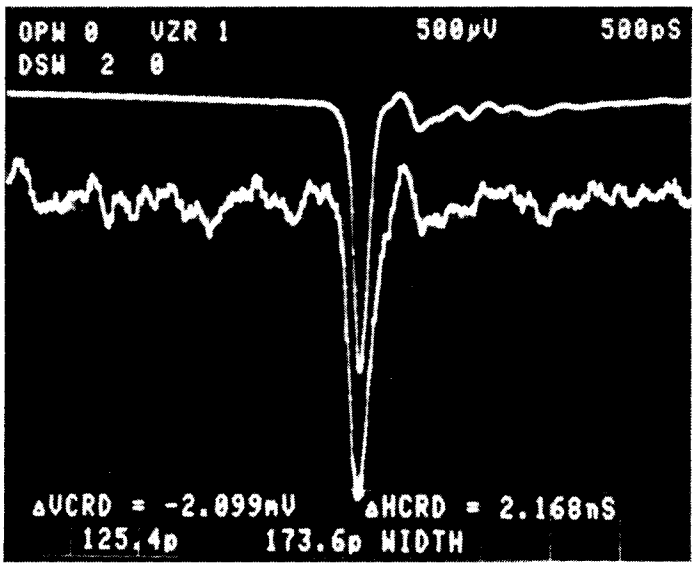

Fig. 14. High speed modulator response.[25] Upper trace is electrical drive pulse; lower trace is transmitted optical power.

laser diode.

The best pulses obtained are shown in Fig. 12. These pulses are 1.6 ps long and represent almost an order of magnitude improvement over the best previous results for a regular pulse train. They are still ~5 times wider than the transform limit for the observed ~30 Å bandwidth. This indicates that considerable amplitude or frequency structure must be present in the pulses.

Good mode-locking was observed only when the laser was operated close to threshold. This is because the light was focused so tightly on the absorber that saturation took place at low light levels. This tight focusing was necessary to obtain a sufficiently fast diffusion-dominated absorption recovery time. In order to mode-lock the laser far above threshold, it is necessary to find a different technique for speeding up the absorption recovery time.

A series of experiments has been performed with proton-bombarded MQW samples.[38] It was found that it is possible to reduce the recovery time by over two orders of magnitude without greatly affecting the other desirable properties of the material. In particular, MQW samples have been produced with recovery times as short as 150 ps which show nonlinear coefficients per excited carrier pair essentially the same as the unbombarded material. Such material should prove to be a versatile and efficient saturable absorber. Experiments are now under way to study diode mode-locking with proton-bombarded MQW samples.

5.3. Modulators

High speed optical modulators have been demonstrated using the QCSE with GaAs/AlGaAs MQWs.[23,25] These modulators rely on the shift of optical absorption with field. For example, we may choose to operate at a photon energy just below the band edge at zero field where the material is substantially transparent; then, by turning on the electric field we may shift the absorption down to the operating photon energy. Because the shifted absorption is so large (5×10^3 to 10^4 cm^{-1}), we can achieve substantial modulation with only micrometers of material thickness.

These modulators are made by growing a structure with about 1 μm of undoped quantum wells between two transparent p and n doped regions to form a p-i-n diode.[23] The field is applied perpendicular to the quantum well layers by reverse-biasing the diode. Fields of the order of 10 kV/cm therefore can be applied with about a volt of bias. Figure 13 shows the schematic structure of a high speed modulator device.[25] Because the material is grown on an opaque GaAs substrate, this has to be removed chemically, as shown. The thickness of the remaining epitaxial semiconductor layers is approximately 4 μm.

The time response of this device is shown in the sampling oscilloscope traces of Fig. 14. The electrical drive (upper trace) has a deconvolved full width at half maximum (FWHM) of 122 ps and an amplitude of 8.5 V. The lower trace shows the transmitted optical power from a GaAs laser diode; it has a deconvolved FWHM of 131 ps. This response is consistent with the RC time constant of the package (capacitance 1.3 pF, drive impedance 50 Ω) and the electrical drive. Faster response is therefore expected for improved packaging of smaller devices.

These modulators, therefore, represent a new approach in optical modulation. They can be physically small, require only moderate electrical drive voltages, and hence have low drive energies. They are compatible with low power semiconductor electronics in drive requirements and also in materials. They are also compatible with laser diodes in operating wavelengths and materials and are capable of high speed modulation.

5.4. Self-electro-optic effect devices

The p-i-n structure used to demonstrate QCSE modulators above also can be operated as a photodetector. Empirically, it is found that for every photon absorbed in the quantum wells a carrier can flow round an external electrical circuit, i.e., the internal quantum efficiency is unity within experimental error[29]; this is what would be expected for absorption within the depletion region of a diode. One important consequence of this is that the same device can operate simultaneously as a modulator and a photodetector. Therefore, if we choose the external electrical circuit appropriately, we can use this to advantage to construct an optoelectronic feedback loop; this is the principle exploited in the self-electro-optic effect device (SEED).[24,26] Depending on whether the feedback is positive or negative, different novel optical devices result. With positive feedback, a low energy optically bistable switch results,[24] and with negative feedback, the

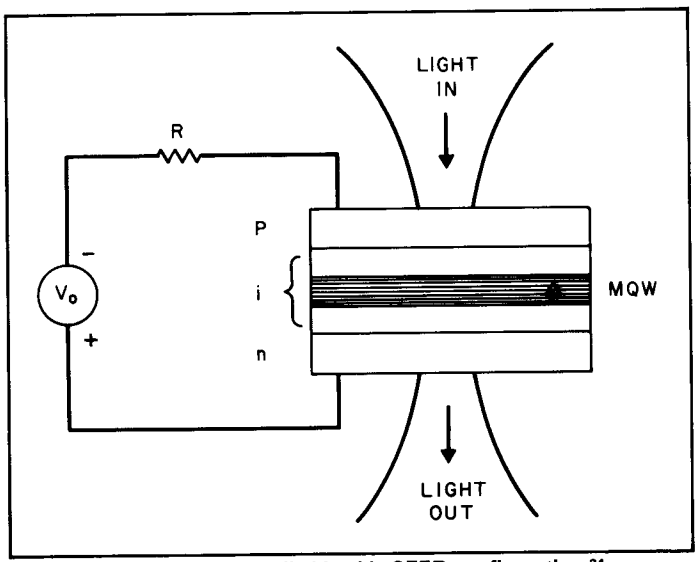

Fig. 15. Schematic of optically bistable SEED configuration.[24]

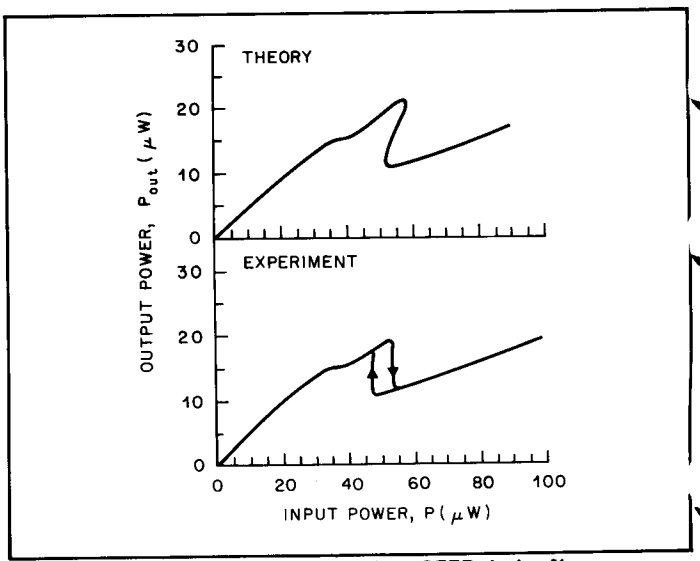

Fig. 16. Optically bistable operation of the SEED device.[24]

device can function as a self-linearized modulator or an optical level shifter.[26] Although the SEEDs are hybrid devices in that they use both optics and electronics for their operation, the ability to have the detector and modulator in the same integrated structure means that the electronics can be minimal (e.g., a resistor[24] or a photodiode[26] and a power supply), and the extremely low energy requirements of the QCSE modulator can give these devices exceptionally low operating energies for devices with both optical inputs and outputs.

The first such SEED to be demonstrated was the optically bistable system shown schematically in Fig. 15. In this case, the operating wavelength is chosen near the main exciton peak position for zero field so that for increasing field (i.e., increasing reverse bias on the diode) the absorption decreases as the exciton moves to lower energy. When no light is shining on the device, there is negligible current, and the full supply voltage reverse-biases the device so that the absorption is relatively low. With increasing incident light, the resulting photocurrent causes a voltage drop across the resistor, and the voltage across the diode decreases, resulting in increased absorption and hence increased photocurrent. Thus, a positive feedback is established, and under the right conditions this can lead to switching into a high absorption state with the exciton shifted right back to the operating wavelength. This leads to the bistable optical input/output characteristic shown in Fig. 16. This bistability belongs to a recently identified general class of optical bistability without mirrors that actually has been observed in many diverse physical systems.[39] A theoretical curve based on this theory and the measured transmission and responsivity of the device is also shown in Fig. 16.

This device is of interest for two reasons. First, it operates under reasonably practical conditions: it runs at room temperature; it requires no cavity or other external feedback; it is compatible with laser diode wavelengths and powers; it can operate over a wide range of time scales and powers [powers as low as 670 nW have been demostrated, and speeds as fast as 400 ns have been tested directly (with a reciprocal relationship between power and speed), with faster operation anticipated for smaller devices]; it can even operate with incoherent light. Second, however, it offers extremely low switching energy per unit area (20 fJ/μm^2 total); this is a factor of six smaller than any other device operating at a comparable wavelength, despite the fact that it uses no resonant cavity to reduce switching energy.

To operate the device in a negative feedback mode, the operating wavelength is chosen somewhat below the band edge so that increasing voltage across the device gives increasing absorption. A particularly interesting device results if the device is biased by a current source.[26] The negative feedback now acts to stabilize the system, and the result is that the device now attempts to set the photocurrent equal to the bias current. Because the photocurrent is exactly proportional to the absorbed power, the result is that the absorbed power is proportional to the bias current. Thus, we have a "self-linearized modulator" exactly linear in bias current drive despite the fact that the voltage modulation function of the device is far from linear. A simple current source is a reverse-biased photodiode illuminated by a second beam of light; the current from this photodiode is proportional to the light shining on it. Hence, it is possible to make a linear inverting, light-by-light modulator, with the power subtracted from the main beam being proportional to the power shining on the separate photodiode.

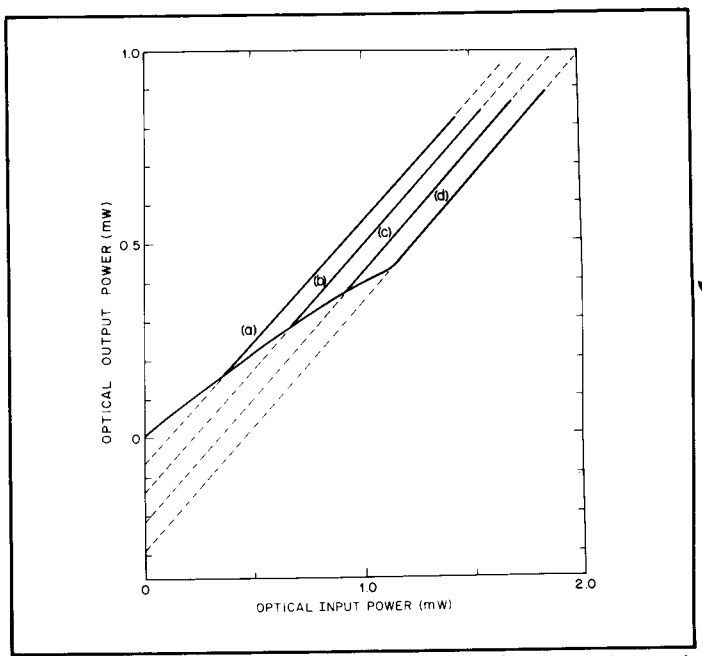

Fig. 17. Optical level shifter action for a SEED under constant current bias of (a) 50, (b) 100, (c) 150, and (d) 200 μA at 858 nm.[26]

Another application of this current-biased negative feedback is as an optical level shifter. This system will subtract a constant optical power, or "baseline," from an incident optical signal. The power subtracted is simply proportional to the current bias of the device. Operation in this mode is illustrated in Fig. 17. Eventually, at low powers a knee is reached in the characteristic because the device cannot increase its absorption any further.

The SEEDs illustrated here serve as examples of the versatility of the QCSE devices. Doubtless, many other devices are possible, and they are particularly attractive because of their practical operating conditions.

6. FUTURE PROJECTIONS

We have described in this paper some ways in which multiple quantum well material can be tailored to have the desired combination of optical properties. Not only does this material exhibit large and fast-responding optical nonlinearities compatible with laser diode outputs, but it also shows large electroabsorption compatible with low power electronic drives; these features make it an attractive choice for many future applications in optical switching and signal processing. The fact that the material and growth techniques are the same as for laser diodes and detectors makes it possible to envisage true integrated optoelectronic circuits in which any combination of lasers, modulators, optical or electronic signal processing elements, and detectors is fabricated on the same semiconductors substrate. It may also be possible to fabricate hybrid electronic/optical circuits in which GaAs electronic circuits are combined with optical signal processing.

Future work will include the extension of these studies into the infrared region of the spectrum (1.3 to 1.6 μm), where optical fiber transmission is most effective, the development of material with recombination centers distributed in such a fashion as to minimize the response time of saturation effects while maximizing the nonlinear response, and the demonstration of further novel modulator and hybrid optoelectronic devices such as the SEEDs. Clearly, much work remains to be done before the full potential of multiple quantum well material is realized, but the rapid progress of the optical phenomena discussed in this paper is very encouraging for future developments.

7. ACKNOWLEDGMENTS

This short review summarizes work performed by our many collaborators and ourselves. We are pleased to acknowledge the invaluable contributions of C. A. Burrus, A. Y. Cho, T. C. Damen, M. C. Downer, D. J. Eilenberger, R. L. Fork, A. C. Gossard, W. H. Knox, A Pinczuk, C. V. Shank, D. Sivco, Y. Silberberg, R. Sooryakumar, B. Tell, W. T. Tsang, J. S. Weiner, W. Wiegmann, T. H. Wood, and J. E. Zucker.

8. REFERENCES

1. R. S. Knox, in Solid State Phys. Suppl. 5, Academic Press, N.Y. (1963).
2. See, for example *Excitons,* E. I. Rashba and M. D. Struge, eds., Modern Problems in Condensed Matter Science Series, North-Holland Pub. Co., Amsterdam (1982).
3. D. S. Chemla and A. Maruani, Prog. in Quantum Electron. 8, 1 (1983).
4. A. C. Gossard, in *Thin Films Preparation and Properties,* K. N. Tu and R. Rosenberg, eds., p. 13, Academic Press, N.Y. (1983).
5. R. Dingle, in *Festkorperprobleme XV,* H. J. Queiser, ed., p. 21, Pergamon/Vieweg, Braunschweig (1975).
6. See, for example, *Device and Circuit Applications of III-V Semiconductor Superlattices and Modulation Doping,* R. Dingle, ed., Academic Press, N.Y. (1985).
7. See, for example, Surf. Sci. 142, 1 (1984).
8. D. S. Chemla, Helv. Phys. Acta 56, 607 (1983).
9. J. E. Zucker, A. Pinczuk, D. S. Chemla, A. C. Gossard, and W. Wiegmann, Phys. Rev. B:29, 7965 (1984).
10. D. A. B. Miller, D. S. Chemla, P. W. Smith, A. C. Gossard, and W. Tsang, Appl. Phys. B:28, 96 (1982).
11. J. S. Weiner, D. S. Chemla, D. A. B. Miller, T. H. Wood, D. Sivco, and A. Y. Cho, Appl. Phys. Lett. 46, 619 (1985).
12. D. A. B. Miller, D. S. Chemla, D. J. Eilenberger, P. W. Smith, A. C. Gossard, and W. T. Tsang, Appl. Phys. Lett. 41, 679 (1982).
13. H. Haug and S. Schmitt-Rink, Prog. Quantum Electron. 9, 3 (1984).
14. D. S. Chemla, D. A. B. Miller, P. W. Smith, A. C. Gossard, and W. Wiegmann, IEEE J. Quantum Electron. QE-20, 265 (1984).
15. S. Schmitt-Rink and C. Ell, *Proc. Third Trieste IUPAP Semiconductor Symposium,* M. H. Pilkuhn, ed., p. 585, North-Holland Pub. Co., Amsterdam (1985).
16. D. A. B. Miller, D. S. Chemla, D. J. Eilenberger, P. W. Smith, A. C. Gossard, and W. Wiegmann, Appl. Phys. Lett. 42, 925 (1983).
17. R. L. Fork, C. V. Shank, C. Hirlimann, and R. Yen, Opt. Lett. 8, 1 (1983).
18. W. H. Knox, M. C. Downer, R. L. Fork, C. V. Shank, Opt. Lett. 9, 522 (1984).
19. W. H. Knox, R. L. Fork, M. C. Downer, D. A. B. Miller, D. S. Chemla, C. V. Shank, and A. C. Gossard, *Proc. Ultrafast Phenomena Conf.,* pp. 162-165, Springer-Verlag, N.Y. (1984).
20. W. H. Knox, R. L. Fork, M. C. Downer, D. A. B. Miller, D. S. Chemla, C. V. Shank, and A. C. Gossard, Phys. Rev. Lett. 54, 1306 (1985).
21. S. Schmitt-Rink, D. S. Chemla, and D. A. B. Miller, unpublished.
22. D. A. B. Miller, D. S. Chemla, T. C. Damen, A. C. Gossard, W. Wiegmann, T. H. Wood, and C. A. Burrus, Phys. Rev. Lett. 53, 2173 (1984).
23. T. H. Wood, C. A. Burrus, D. A. B. Miller, D. S. Chemla, T. C. Damen, A. C. Gossard, and W. Wiegmann, Appl. Phys. Lett. 44, 16 (1984).
24. D. A. B. Miller, D. S. Chemla, T. C. Damen, A. C. Gossard, W. Wiegmann, T. H. Wood, and C. A. Burrus, Appl. Phys. Lett. 45, 13 (1984).
25. T. H. Wood, C. A. Burrus, D. A. B. Miller, D. S. Chemla, T. C. Damen, A. C. Gossard, and W. Wiegmann, IEEE J. Quantum Electron. QE-21, 117 (1985).
26. D. A. B. Miller, D. S. Chemla, T. C. Damen, T. H. Wood, C. A. Burrus, A. C. Gossard, and W. Wiegmann, Opt. Lett. 9, 567 (1984).
27. See, for example, G. E. Stillman and C. M. Wolfe, in *Semiconductors and Semimetals,* R. K. Willardson and A. C. Beer, eds., p. 380, Academic, New York (1977).
28. J. D. Dow and D. Redfield, Phys. Rev. B:1, 3358 (1970).
29. D. A. B. Miller, D. S. Chemla, T. C. Damen, A. C. Gossard, and W. Wiegmann, Opt. Lett. 9, 567 (1984).
30. D. A. B. Miller, D. S. Chemla, P. W. Smith, A. C. Gossard, and W. Wiegmann, Opt. Lett. 8, 477 (1983).
31. E. P. Ippen, D. J. Eilenberger, and R. W. Dixon, Appl. Phys. Lett. 37, 267 (1980).
32. H. Yokoyama, H. Ito, and H. Inaba, Appl. Phys. Lett. 40, 105 (1982).
33. J. P. van der Ziel, W. T. Tsang, R. A. Logan, R. M. Mikulyak, and W. M. Augustyniak, Appl. Phys. Lett. 39, 525 (1981).
34. C. Harder, J. S. Smith, K. Y. Lau, and A. Yariv, Appl. Phys. Lett. 42, 772 (1983).
35. H. A. Haus, IEEE J. Quantum Electron. QE-11, 736 (1975).
36. G. H. C. New, IEEE J. Quantum Electron. QE-10, 115 (1979).
37. Y. Silberberg, P. W. Smith, D. J. Eilenberger, D. A. B. Miller, A. C. Gossard, and W. Wiegmann, Opt. Lett. 9, 507 (1964).
38. Y. Silberberg, P. W. Smith, D. A. B. Miller, B. Tell, A. C. Gossard, and W. Wiegmann, Appl. Phys. Lett. 46, 701 (1985).
39. D. A. B. Miller, J. Opt. Soc. Am. B. 1, 857 (1984).